

SIMULATION OF DROPWISE CONDENSATION UNDERNEATH A CHEMICAL TEXTURED SUBSTRATE WITH A WETTABILITY GRADIENT

Basant Singh Sikarwar

Department of Mechanical Engineering
Indian Institute of Technology Kanpur
Kanpur 208016, India
sikarwar@iitk.ac.in

Sameer Khandekar*

Department of Mechanical Engineering
Indian Institute of Technology Kanpur
Kanpur 208016, India
samkhan@iitk.ac.in

K. Muralidhar

Department of Mechanical Engineering
Indian Institute of Technology Kanpur
Kanpur 208016, India
kmurli@iitk.ac.in

(*Corresponding Author)

ABSTRACT

In applications such as dropwise condensation and a laboratory-on-a-chip device, it is required to move a liquid drop that is located on or underneath a solid surface. The speed of response on one hand, and the smallest drop size at which motion is enabled on the other, determine the device efficiency. Spontaneous movement of micro-droplets on a horizontal surface by suitable variable-surface-energy coatings, which introduce a wettability gradient, is a promising technique for droplet motion, as compared to other methods suggested in the literature.

Dropwise condensation of water underneath a horizontal surface having a unidirectional constant wettability gradient is numerically modeled in the present work. Simulation data have been compared with condensation patterns for a horizontal surface and an inclined surface, both with zero wettability gradients. The mathematical model includes nucleation, growth by vapor condensation and coalescence, and drop instability arising from force imbalances at the three-phase contact line. Results obtained show that wettability gradient can effectively control the condensation process by diminishing the cycle time of nucleation, growth and removal.

INTRODUCTION

Pure vapor condenses in a heterogeneous manner when it contacts a solid surface held below the saturation temperature. Dropwise, filmwise and mixed mode condensations are possible. Heat transfer coefficient for dropwise condensation can be up to an order of magnitude larger than filmwise

condensation [1]. This stems from the fact that the absence of condensate film and continuous surface renewal by sliding/falling large drops reduce the thermal resistance and improve heat transfer. Any method of enhancing heat transfer coefficient is naturally desirable for improving system efficiency [2]. Hence, dropwise condensation is attractive for enhancement of heat transfer in a variety of applications.

Although dropwise condensation has been a subject of interest, the mechanism of dropwise condensation is not yet fully clear. Much of the literature suggests that droplets form at individual nucleation sites, while the area between them is regarded inactive with respect to condensation [3-4]. As drops grow in size, conduction resistance increases while the rate of condensation on the exposed surface decreases [5]. Beyond a certain point, drops grow mainly by coalescence. At a certain size, drops slide off (or fall off) and re-expose the substrate for fresh nucleation. This cyclic sweeping process and generation of small droplets leads to a large heat transfer coefficient (Figure 1, [6]).

The timescale of drop instability can be controlled by altering the surface characteristics [7]. A simple approach for mobilization of drops is to incline the surface with respect to horizontal. The focus of the present study is on horizontal surfaces and motion can be initiated on it as follows [8-9]: (i) apply a temperature gradient on the substrate so that Marangoni motion is initiated and (ii) create surface energy gradients on the substrate by suitable physico-chemical treatment.

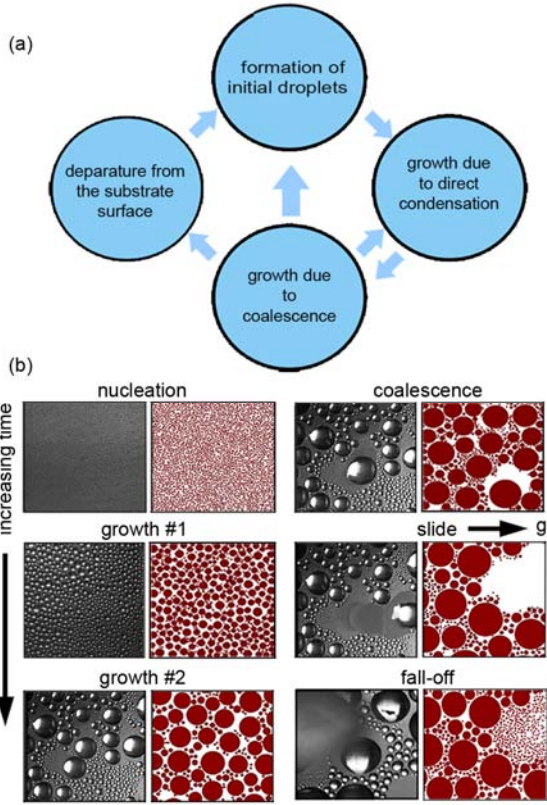


Figure 1: Complete cycle of dropwise condensation as observed in experiment and in simulation [6].

The second approach is quite possible by depositing organic long chain monolayers over polymeric or glass surfaces [10-11]. Denial et al. [12] reported that a small drop (1 to 2 μ l) could slide with high velocity (0.15 to 1.5 m/s) on a substrate with a wettability gradient. Moumen et al. [13] recorded video images of drop motion and analyzed the relationship between drop size and velocity as functions of local wettability.

Dropwise condensation of water underneath a horizontal surface with a unidirectional linear wettability gradient is numerically modeled in the present work. The mathematical model includes nucleation, growth by direct condensation, coalescence, and drop instability arising from force imbalances. Simulation data have been compared with condensation patterns for a flat surface with zero-gradient and one with a small inclination. The changes in overall cycle-times during the condensation process due to wettability-gradient of the surface are reported.

MODEL DEVELOPMENT

The model presented here is a variant of an earlier work of the authors [14] wherein dropwise

condensation process underneath an inclined, chemical textured substrate was considered. There are significant differences, however. A horizontal substrate with a wettability gradient underneath it, which facilitates spontaneous droplet motion, is shown in Figure 2. Here, the drop is deformed due to variation of wettability on the substrate, Figure 2b. The shape of the contact line (droplet base) is assumed to be circular and the relevant forces that move the drop towards the hydrophilic region of the substrate is highlighted in Figure 2c.

For calculation of volume and surface area of the deformed drops, their surfaces are fitted by a spherical cap, which is the shape assumed by a small static drops in the absence of a gravitational effect, Figure 2b. The average contact angle due to the spherical cap approximation is given by:

$$\theta_{avg} = \left(\frac{\theta_{max} + \theta_{min}}{2} \right) \quad (1)$$

The drop volume V , area of liquid-vapor interface A_{lv} and area of solid-liquid interface A_{sl} are expressed by the following equations:

$$V = \frac{\pi r^3}{3} (2 - 3 \cos \theta_{avg} + \cos^3 \theta_{avg}) \quad (2)$$

$$A_{lv} = 2\pi r^2 (1 - \cos \theta_{avg}) \quad (3)$$

$$A_{sl} = \pi r^2 (1 - \cos^2 \theta_{avg}) \quad (4)$$

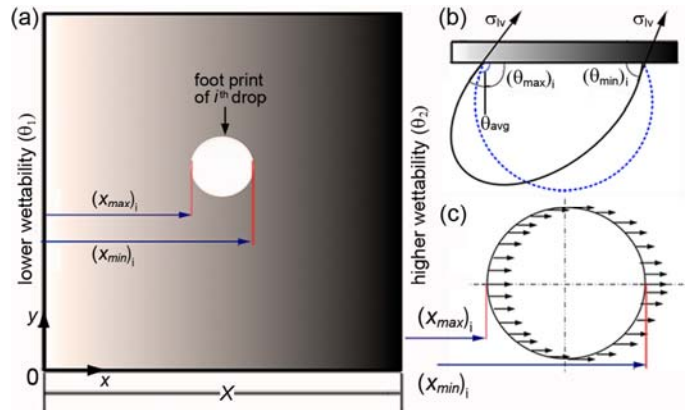


Figure 2: (a) A substrate with wettability gradient. The footprint of i^{th} drop assumed circular. (b) Side view of i^{th} drop and its approximate hemispherical shape (c) direction of force acting at the three phase contact line at substrate with wettability gradient.

In the present simulation, the contact angle at the non-wetting side ($x = 0$) is taken as $\theta_1 = 120^\circ$, while that at the higher wettability side ($x = X$), $\theta_2 = 96^\circ$. The contact angle is taken to vary linearly in one direction from $x = 0$ to X , as follows:

$$\theta = \theta_1 - \left(\frac{\theta_1 - \theta_2}{X} \right) \cdot x \quad (5)$$

Here, the drop size $X = 30$ mm. The x coordinate over the periphery of the drop and the contact angle difference between the trailing and leading edges is required to be calculated at each time step and each drop.

The area of condensation is chosen as a square of size $30 \text{ mm} \times 30 \text{ mm}$. Condensation is initiated by nucleation at 9×10^7 points over this site corresponding to a nucleation site density of 10^9 sites per cm^2 . This number is commonly encountered in engineered surfaces used in heat exchangers. The nucleation sites are distributed over the area by using a random number generator function in C++ that returns a matrix containing pseudo random number with a uniform probability density function in the range $[0, 1]$. The distribution proceeds column-wise till all the sites are occupied. The drops are assigned the minimum diameter derived from thermodynamic considerations. Subsequently, they grow with time, the first phase of growth being controlled by direct condensation of vapor. The smallest radius of the droplet located at each nucleation site is given by thermodynamic considerations as:

$$r_{\min} = \frac{2\sigma v_l T_w}{H_{lv} [T_{sat} - T_w]} \quad (6)$$

The drop growth rate at each nucleation sites by direct condensation is [14]:

$$\frac{dr}{dt} = \frac{4\Delta T_t}{\rho_l H_{lv}} \left[\frac{\left(\frac{1 - r_{\min}}{r} \right)}{\frac{2}{h_{int}} + \frac{r}{k_c}} \right] \left[\frac{(1 - \cos \theta_{avg})}{(2 + 3 \cos \theta_{avg} - \cos^3 \theta_{avg})} \right] \quad (7)$$

Here, interfacial heat transfer coefficient h_{int} is derived from kinetic theory of gases [1] and is expressed as:

$$h_{int} = \left(\frac{2\hat{\sigma}}{2 - \hat{\sigma}} \right) \left(\frac{H_{lv}^2}{T_s v_{lv}} \right) \left(\frac{\bar{M}}{2\pi \bar{R} T_s} \right)^{1/2} \quad (8)$$

When two drops touch each other, they are replaced by a drop of equal volume, placed at their resultant center of mass. The distance between two nucleation sites on the substrate, i and j , is calculated by following equation:

$$d_{ij} = \sqrt{(x_i - x_j)^2 + (y_i - y_j)^2 + (z_i - z_j)^2} \quad (9)$$

Therefore, the coalescence criterion for the present study is stated as:

$$d_{ij} - (r_i + r_j) < 10^{-3} \quad (10)$$

The drops are allowed to grow by direct condensation as well as coalescence. The active and inactive nucleation sites are verified after the coalescence.

Next, we estimate the force exerted by the substrate on the drop at the contact line due to differences in contact angle (namely, contact angle hysteresis, $\Delta\theta$). For this step, consider i^{th} drop top view of the footprint, assumed to be a circle is used, Figure 2(a-c). From Figure 2(c), it can be seen that the net contact line force that acts on the i^{th} drop in the x direction can be calculated as follows:

1. Calculate the base radius of the drop. This is equal to the radius calculated at the previous step plus the effect of the growth rate of the drop (direct condensation plus coalescence).

2. Calculate the x_{\min} and x_{\max} for the i^{th} drop. After knowing these values, the value of $(\theta_{\max})_i$ and $(\theta_{\min})_i$ are calculated as:

$$(\theta_{\max})_i = \theta_1 - \left(\frac{\theta_1 - \theta_2}{X} \right) (x_{\max})_i \quad (11)$$

$$(\theta_{\min})_i = \theta_1 - \left(\frac{\theta_1 - \theta_2}{X} \right) (x_{\min})_i \quad (12)$$

3. The variation of contact angle at footprint of i^{th} droplet is given by:

$$(\theta_x)_i = (\theta_{\max})_i + \frac{\pi - \{(\theta_{\min})_i + (\theta_{\max})_i\}}{[(x_{\min})_i - (x_{\max})_i]} x \quad (13)$$

4. The net force acting in the x direction on the i^{th} drop is:

$$(F_x)_i = 2\pi\sigma_{lv} (r_b)_i \int_{(x_{\max})_i}^{(x_{\min})_i} \cos(\theta_x)_i dx \quad (14)$$

Hence

$$(F_x)_i = 2\pi\sigma_{lv} (r_b)_i \frac{X}{(\theta_1 - \theta_2)} [\sin(\theta_{\max})_i - \sin(\theta_{\min})_i] \quad (15)$$

The hydrodynamic force which acts to oppose the motion of the i^{th} drop is:

$$(F_{hyd})_i = C_f (0.5\rho U_i^2) (A_{sl})_i \quad (16)$$

The skin coefficient of friction C_f is taken as:

$$C_f = 58 \text{ Re}^{-0.97} (\theta_{avg})_i^{-1.58} \quad (17)$$

By setting the net force exerted by the solid on the fluid in the horizontal direction $F_{x,i} + F_{hyd} = 0$, a

result can be obtained for the terminal speed of each drop in the form:

$$U_i = \left[\frac{0.044 \cdot (F_x)_i (\theta_{avg})_i^{1.58}}{\rho^{0.03} \mu^{0.97} (d_b^{1.03})_i} \right]^{1/1.03} \quad (18)$$

Similarly, the critical velocity of each drop at its individual stage of growth is determined. Each drop moves towards the higher wettability side while the velocity of sliding depends on the base radius of the drop and the average contact angle. As the drops slide over the substrate, hidden sites underneath the original drop become active and the nucleation process is repeated. As the drop grows, its sliding velocity increases. If the weight of the drop is higher than the net retention force normal to the plane due to surface tension, it will fall-off. Hence, the falling criterion for the maximum pendant drop size that is gravitationally stable is:

$$(r_{max})_i = \sqrt[3]{\frac{6\sigma_{lv} \sin^3 \theta_{avg}}{\rho g (2 - 3 \cos \theta_{avg} + \cos^3 \theta_{avg})} \left(\frac{X}{\theta_1 - \theta_2} \right)} \left[\cos(\theta_{min})_i - \cos(\theta_{max})_i \right] \quad (17)$$

NUMERICAL ALGORITHM

The important steps of the numerical algorithm are listed here: (i) Initialize all variables and input material properties; (ii) randomly distribute the nucleation sites ($10^9/\text{cm}^2$) on the substrate and place drops of minimum radius at all nucleation sites; (iii) calculate the coordinates of the nucleation site and assign contact angles at each of them; (iv) solve Equation 7 by a 4th order Runge-Kutta method and find the new radius; (v) calculate the base radius of drop and assigned contact angle according to the wettability gradient; (vi) calculate force imbalance and shift the drop towards the region of higher wettability; (vii) calculate the intermediate distance between the nucleation sites; (viii) check for drop coalescence; (ix) identify the sites already covered by drops and make them hidden; (x) search for exposed sites and provide a minimum radius drop on such sites; (xi) check for the critical radius of slide-off and the sliding velocity; (xii) repeat (iii)-(xi) till a dynamic steady-state is reached.

RESULTS AND DISCUSSIONS

Numerical computations are conducted for nucleation site density of $10^9/\text{cm}^2$ on: (i) a substrate with a wettability gradient, (ii) an inclined surface

(5°), and (iii) a horizontal substrate; the latter two substrates having no wettability gradients. More details of modeling dropwise condensation process on horizontal and inclined surfaces are available in [14]. Condensation of water occurs on the underside of the substrate of size 30 mm × 30 mm; drops are taken to be in the pendant mode at all times. For the present simulation, the degree of subcooling is $\Delta T_{\text{sat}} = 5^\circ\text{C}$ with a saturation temperature of 27°C .

Simulations show that the model presented above captures the inherent mechanism of dropwise condensation over a surface with a wettability gradient. The features of the condensation cycle are similar to those of an inclined surface shown in Figure 1. Figure 3 show the temporal-spatial drop distribution underneath a horizontal substrate with wettability gradient. The points of difference for a graded surface are: (i) drops shift towards the higher wettability side, (ii) drops of all sizes are in motion, (iii) larger drops acquire greater velocity and (iv) growth and sliding occur simultaneously.

Spatial distribution of drops at an instant just before the first drop leaves the surface on a graded substrate, first slide-off from an inclined substrate and the first fall-off from a horizontal substrate are compared in Figure 4. In view of the motion of drops of every size, there is an exposed virgin area behind every droplet on the graded substrate, as seen in Figure 4a. Hence, the active (exposed) area for a wettability gradient surface is greater than other configurations. This result is summarized in Table 1. The time cycle from initial nucleation to the instant when the drop leaves the surface is also given in Table 1. It is a minimum for the surface with a wettability gradient.

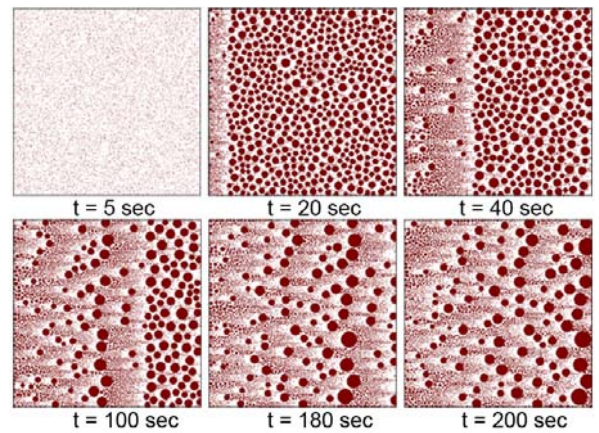


Figure 3: Temporal-spatial drop distribution underneath a horizontal substrate with a wettability gradient.

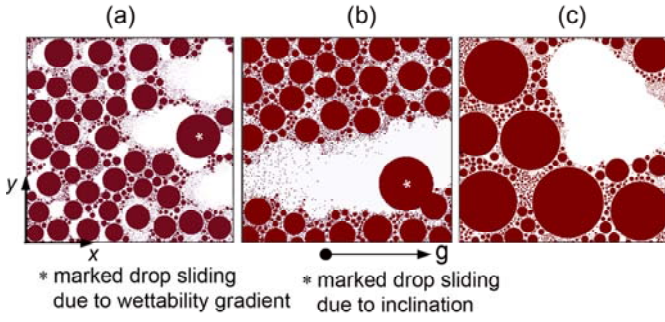


Figure 4: Droplet motion underneath a chemically textured substrate with (a) wettability gradient imposed on a horizontal substrate, (b) inclined substrate (5°) with no wettability gradient and, (c) a pendant drop fall-off from a horizontal substrate with no wettability gradient.

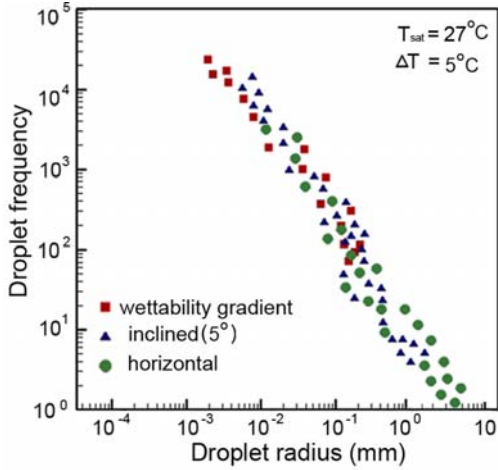


Figure 5: Droplet frequency (the number of drops) as a function of the drop radius, just before the first drop leaves the surface.

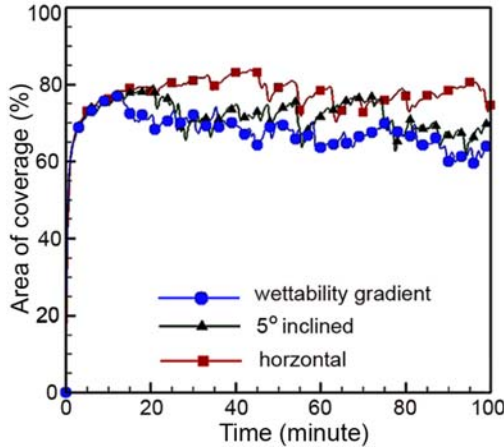


Figure 6: Effect of the choice of the substrate on the percentage area of coverage.

For surfaces with wettability gradient, smaller drops move with small velocity and larger drops with large velocity. For an inclined substrate, only the drop that reaches the critical size is set in motion. For the horizontal surface, there is no sliding motion possible; the drop falls off at criticality. For the surface with a wettability

gradient, the drop may also fall-off due its weight exceeding surface tension. This factor has been included in the simulation. However, for the range of parameters considered, specifically the size of the substrate, fall-off was not realized.

Table 1: Simulation statistics

| Case study | Time of first drop slide/fall-off (leave-off) | Size of drop while leaving the surface | Active area |
|------------------------|---|--|-------------|
| Wettability y gradient | 18 minutes | 2.53 mm | 38% |
| Inclined substrate | 42 minutes | 3.47 mm | 23% |
| Horizontal | 55 minutes | 5.67 mm | 18% |

Figure 5 shows the droplet frequency on the three substrates as a function of drop radius, just before the slide/fall-off criticality is achieved. It is clear that the population of small drops on graded substrate is larger as compared to the other two.

Figure 6 shows the area of coverage with respect to time. It is seen that the area coverage for the graded surface is smaller, making the exposed virgin area larger than the other two surfaces. Consequently, the heat transfer coefficient can be expected to be the greatest for a surface with variable wettability. It is also seen that incipience of droplet slide-off event is at an earlier time instant on the graded surface.

CONCLUSIONS

Simulation of dropwise condensation of water vapor underneath a surface having a wettability gradient is reported, with the following conclusions:

1. Simulation presented herein is sufficient to capture all the major components of the quasi-cyclic dropwise condensation process.
2. Droplets move from a region of lower wettability towards one with higher wettability.
3. On the graded surface, the sliding velocity of drops is a function of its base radius. Larger drops move with higher velocity.
4. The active virgin area for a wettability gradient substrate available for nucleation is greater than what is realized for the other two substrates, i.e. an inclined and a horizontal surface both having uniform wettability.
5. Wettability gradient results in a larger number of small drops and hence will lead to a higher average heat transfer coefficient.

NOMENCLATURE

| | |
|------------|--|
| A | Area of cross-section (m^2) |
| C_f | Skin friction coefficient |
| d | Diameter of the drop (m) |
| F | Force (N) |
| H_{lv} | Latent heat of vaporization (J/kg) |
| h | Heat transfer coefficient ($\text{W}/\text{m}^2\text{-K}$) |
| k_c | Thermal conductivity of condensate ($\text{W}/\text{m-K}$) |
| r | Radius of the drop (m) |
| Re | Reynolds number ($\rho U d_a / \mu$) |
| \bar{R} | Universal gas constant (J/kg-K) |
| T | Temperature (K) |
| ΔT | Temperature difference ($T_w - T_{\text{sat}}$) (K) |
| dt | Time step (s) |
| U | Velocity of the moving drop (m/s) |
| V | Volume of the drop (m^3) |
| x, y, z | Cartesian coordinates |
| X | Size of substrate in the x -direction (m) |

Greek symbols

| | |
|----------------|---|
| α | Inclination angle (deg) |
| μ | Dynamic viscosity (Pa-s) |
| v | Specific volume (m^3/kg) |
| ρ | Density (kg/m^3) |
| σ_{lv} | Surface tension of liquid vapor interface (N/m) |
| $\hat{\sigma}$ | Accommodation coefficient |
| θ | Contact angle (radian or deg) |

Subscripts

| | |
|-----------|--|
| avg | Average |
| b | Base of the drop |
| $crit$ | Critical |
| d | Drop |
| g | Gravity |
| hyd | Hydrodynamic |
| i | Number of droplets; i.e., i^{th} droplets |
| int | Interfacial heat and mass transfer |
| l | Liquid |
| lv | Liquid vapor interface |
| sl | Solid-liquid interface |
| v | Vapor |
| w | Condensing wall |
| x, y, z | Cartesian coordinates |

REFERENCES

- [1] Carey, V. P., *Liquid-vapor phase-change phenomena*, 2nd ed., Hemisphere Publishing Corporation, USA, 1992, pp.413-472.
- [2] Burnside, B. M., and Hadi H. A., 1999. Digital computer simulation of dropwise condensation from equilibrium droplet to detectable size, *International Journal of Heat and Mass Transfer* 42(11), 3137-3146.
- [3] Rose, J. W., 2002. Dropwise condensation: theory and experiments: A review, *Proc. Institution of Mechanical Engineers*, 216, 115-118.
- [4] Leipertz, A., 2010. Dropwise condensation. In: Stephan, P. (Eds.) *VDI Heat Atlas VDI-GVC* (ed. 2), Springer-Verlag, Germany, pp. 933-937.
- [5] Vemuri, S., and Kim, K. J., 2006. An experimental and theoretical study on the concept of drop wise condensation, *International Journal of Heat and Mass Transfer*, 49, 649-657.
- [6] Sikarwar, B. S., Battoo, N. K., Khandekar, S., and Muralidhar, K., 2011. Dropwise condensation underneath chemically textured surfaces: Simulation and experiments, *ASME Journal of Heat Transfer*, 133(2), 021501 (1-15).
- [7] Pratap, V., Moumen, N., and Subramanian, R., 2008. Thermocapillary motion of a liquid drop on a horizontal solid surface, *Langmuir*, 24, 2185-5193.
- [8] Subramanian, R., S., Moumen, N., and McLaughlin, J. B., 2005. The motion of a drop on a solid surface due to a wettability gradient, *Langmuir*, 21, 11844-11849.
- [9] Lan, Z., Ma, X. Z., Zhang, Y., and Zhou X. D., 2009. Theoretical study of dropwise condensation heat transfer: Effect of the liquid-solid surface free energy difference, *Journal of Enhanced Heat Transfer*, 16, 61-71.
- [10] Berthier J., *Microdrops and Digital Microfluidics*, 2nd ed., Hemisphere Publishing Corporation, USA, 2008, pp. 75-179.
- [11] Qiang, L., Hong W., and Xun, Z., Mingwei Z., 2006. Droplet movement on horizontal surfaces with gradient surface energy, *Science in China, Series E: Technological Sciences*, 49(6) 733-744.
- [12] Denial, S., Chaudhury, M. K., and Chen, J. C., 2001. Fast drop movements resulting from the phase-change on a gradient surface, *Science*, 291, 633-636.
- [13] Moumen, N., Subramanian, R. S., and McLaughlin, J. B., 2006. Experiments on the motion of drops on a horizontal solid surface due to wettability gradient, *Langmuir*, 22, 2682-2690.
- [14] Sikarwar, B. S., Khandekar, S., Agrawal, S., Kumar, S., and Muralidhar K., 2012. Dropwise condensation studies on multiple scales, *Heat Transfer Engineering*, 33 (3/4).